International Journal of Innovative Technology and Exploring Engineering (IJITEE)
ISSN: 2278-3075 (Online), Volume-8 Issue-11, September 2019

An Automated System for Identification of Skeletal Maturity using Convolutional Neural Networks Based Mechanism

B Sowmya Reddy, Devavarapu Sreenivasarao, Shaik Khasim Saheb

Abstract*: This paper puts forward a proposition of automated skeletal recognition system that takes an input of left hand-wrist-fingers radiograph and give us an output of the bone age prediction. This system is more reliable, if is successful and time-saving than those laborious, fallible and time-consuming manual diagnostic methods. Here, a Faster R-CNN takes the input of left-hand radiograph giving the detected DRU region from left-hand radiograph. This output is given as an input to a properly trained CNN model. The experiment section provides us with the details regarding the experiments conducted on 1101 radiographs of left hand and wrist datasets and accuracy of model when different optimization algorithms and training sample amounts were utilized. Finally, this proposed system achieves 92% (radius) and 90% (ulna) classification accuracy after the parameter optimization.

Keywords*: About four key words or phrases in alphabetical order, separated by commas.

I. INTRODUCTION

Evaluating and understanding the bone age (the level of bone maturity) of an individual say a child, is very much important since it helps us to put tabs on the possible skeletal disorders and understand the baby spurts and implementing the treatment accordingly [1],[2]-[5]. The aftermath of ignoring the prediction or understanding the bone age could be scoliosis (a medical disorder where the length of the spine shifts sideward) and many other metabolic disorders like hyperthyroidism and diabetes mellitus [6]. This skeletal maturity assessment is done with the help of a left-hand radiograph (wrist, hand and fingers) because these bones look different with age [1]. Classification processes that are widely used these days- Greulich Pyle [7] and Tanner-Whitehouse [8]-[10]. Greulich and Pyle have proposed an atlas that contains the X-rays which are to be matched with the X-Ray image of a child and predict the bone age. Though this method is easier than the Tanner-Whitehouse method which requires a hectic effort where we score 20 complexes of bones that are present in the hand and the wrist, it is presumed to have reliability problems [1]. Luk et al [6], in the year 2013, proposed a simplified version of the TW3 method (a scheme where mineral density of bones is assessed) with the help of (DRU).

Since the DRU area covers the most of the left-hand area, it helps us to assess the bone maturity of the infants and the juvenile people and predicts the accelerating and retarding phases of puberty [13],[14].

Now coming to the models of deep learning, the ANN descendants; and Convolutional Neural Networks, which are proficient in detection and classification of objects. Therefore, the research groups are applying CNNs and the deep learning models for the medical image analysis for the promising results [15]. Say, the classification of the patterns of diseases in lungs.

Here, in this study an automated deep learning based DRU system is proposed. From the radiographic input images, the DRU portion is extracted with the help of Faster R-CNN model (object detection model) and the extracted portion is then fed into the CNN model for the bone age prediction [20]. Experiments were done on different model configurations and the one with the best performance is chosen. Basically, the motives of this experiment are 1) to bring forth a rapid system that is entirely based on the CNNs to estimate the skeletal maturity. 2) to improve the performance of models using the balancing, augmentation and optimizing data techniques.

II. RELATED WORK

In the above section we crossed paths with the shortcomings of the GP and TW3 methods. Tristan-Vega and Arribas. [21], brought a technique for end to end automation system introduced in the year 2008. This method is mainly for the prediction of skeletal maturity in Childs. The procedure works with a segmentation algorithm dealing with clustering. The segmentation phase in general segment the bones there after it develops a GSP network. This process results into an assessment or prediction of bone maturity.

On the other hand, Liu et al. [22] introduced an ANN method which consists of feed-forward multi-layers is used in estimation of bone age with the usage of left-hand-wrist radiographs.

Manuscript published on 30 September 2019.
*****Correspondence Author(s)
B Sowmya Reddy is currently pursuing B.Tech Degree program in Computer Science & Engineering in Sreenidhi Institute of Science and Technology, Affiliated to Jawaharlal Nehru Technical University Hyderabad, Telangana, India, PH-8500038470. E-mail: sowmyareddy0711@gmail.com
Devavarapu Sreenivasarao is currently working an Assistant Professor in Computer Science & Engineering Department in Sreenidhi Institute of Science and Technology and his area research includes Medical Image Processing, Machine Learning. PH-9866014581. E-mail: sreenivasaraodevavarapu@gmail.com
Shaik Khasim Saheb is currently working as Assistant Professor in Computer Science & Engineering Department in Sreenidhi Institute of Science and Technology, and his area research includes Medical Image Processing, Machine Learning. PH-9642097865. E-mail: shaikkhasims@sreenidhi.edu.in

In one of the papers Somkantha et al. [23] proposed boundary information in which the features of boundary were fully processed in correspondence with Support Vector Regression of carpal bone image X-Ray in assessing the bone.
In the paper Lin et al. [24], implemented a technique called FNN which is completely based on Cluster for assessment of bone.
In the paper Soek et al. [25] introduced one other automated system for determining the bone age with the help of left hand-wrist radiographs. Upon usage of Scale Invariant Feature Transform (SIFT), initially the positional features are identified in the given input images. There after a Singular Value Decomposition technique which is based on feature vectors implemented in order to represent the features. And finally, these feature vectors which are obtained in the earlier step can be given input to the Neural Networks in prediction of bone age.
In one of the paper Davis et al. [26] implemented a decision tree method which is used to estimate bone age upon consideration of radiographic features in addition to that the ages are also being predicted by using a technique called as TW3.
In one of the papers Harmsen et al. [27] constructed a model which is based on SVM. This model is then tested by comparison of k-Nearest Neighbor (k-NN).
In one of the paper Cunha et al. [28] implemented a technique in order to improve bone age prediction and they named the technique as ensemble technique. The aim of this technique is to extract various features from joints of fingers and also these feature descriptors are merged with the ensemble technique in prediction of bone age.
In one of the papers Ebner et al. [29] implemented a method which is random regression forests in predicting the bone age. All these above methods, though are successful, but aren't automated systems therefore a completely automated deep learning methods which are deemed and then be used in medical analysis applications [19].

III. DATA AND METHOD

A. PREPARATION OF THE DATA

The input radiographs of the hand-wrist for this experiment were collected from adolescent idiopathic scoliosis patients who were getting treated in a tertiary scoliosis clinic. 400 radius and 600 ulnas were retrieved from alike looking left-hand radiographs that differ with respect to the position and resolution (Fig 1).

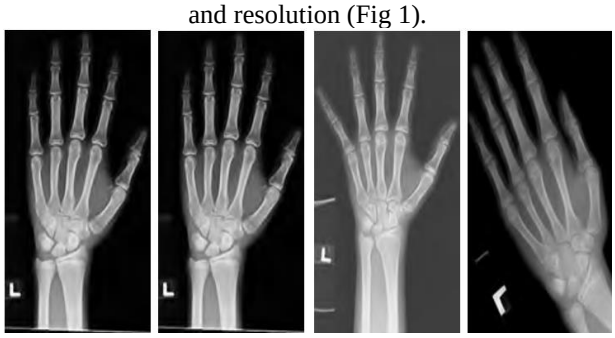

Fig 1: Left hand radiographs with respect to different positions and resolutions

In the (Fig 2), the R1-R11 grading of DRU was displayed. Different radiographs were collected from different positions and epiphysis maturity stages (Sitting Height, Tibia Length Standing Height, Radius and Arm Span) [11],[12].

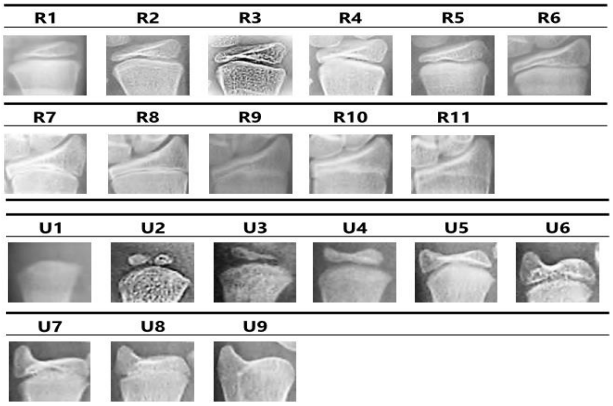

Fig 2: Radius and ulna samples with age.

(Fig 3) shows the grades of ulna and radius development at various stages. It gives us the overview of radius and ulna during their epiphyseal fusion states and the overview of bones when the child reaches skeletal maturity (at around 18 to 25 years of age), a stage where the bones at the rounded ends replace all the cartilage sheathing them earlier.

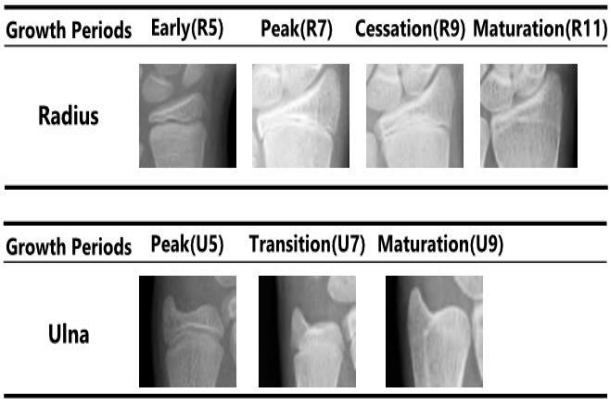

Fig 3: Epiphysis and maturity stage's version of Radius and Ulna

Data distribution of Radius: R5 stage provides the early growth period with 33 and R6 provides the same period with 42 images. Similarly, R7 provided the peak growth period with 75 and R9 provided the growth cessation category with 175 images respectively and R11 stage provided 75 images for maturation period. Therefore, from a total of 400 images, 100 are randomly selected testing images and the other 300 are training images. Data distribution of Ulna: U4 and U5 stages provided 191 images and 9 from the U6 which are similar to the U5 stage. These 200 images were categorized under a period named early growth. U7 provided 250 images to represent growth transition period. Similarly, U9 and U8 stages provided 138 and 12 images respectively and are constructed under growth maturation period samples. A total of 600 images, of which 150 are testing samples and 450 are training samples.

B. AUGMENTATION OF DATA AND SAMPLE BALANCING

Neural networks are effective, when trained with categories containing more samples. But that is not the case with this, since it consists a group of 1000 images in the dataset. In training dataset. And (table 1) shows the radius data distribution. It is clear that the distribution of data is uneven. Therefore, using oversampling, the data in each group was made to be 150. Similarly, in data distribution of ulna (table 2), data was balanced to be 200 in each group.

To avoid the over-fitting issues, we augment the data, translating and rescaling to enlarge the training dataset. (Fig 4) shows the distribution of data in the radius and ulna.

Bone Age Periods(Ulna)	Peak	Transition	Maturation	Total
Original Training Data	150	200	100	450
After Data Balance	200	200	200	600
After Data Augmentation	1000	1000	1000	3000

Table 1: Radius data distribution

Bone Age Periods(Radius)	Early	Peak	Cessation	Maturation	Total
Original Training Data	50	50	150	50	300
After Data Balance	150	150	150	150	600
After Data Augmentation	750	750	750	750	3000

Table 2: Ulna data distribution

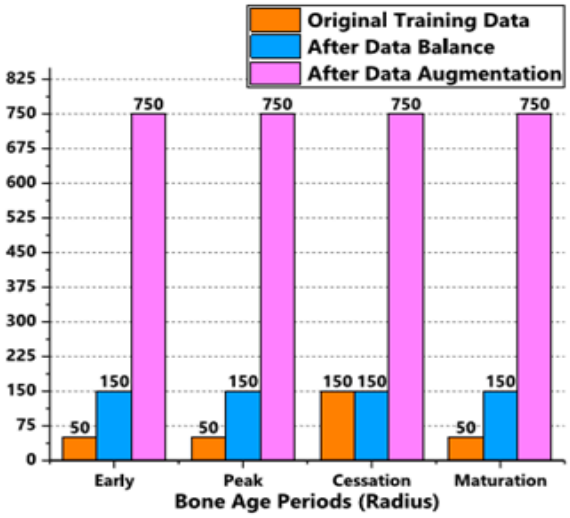

Fig 4(a): Data distributions after data balancing and augmentation (Radius)

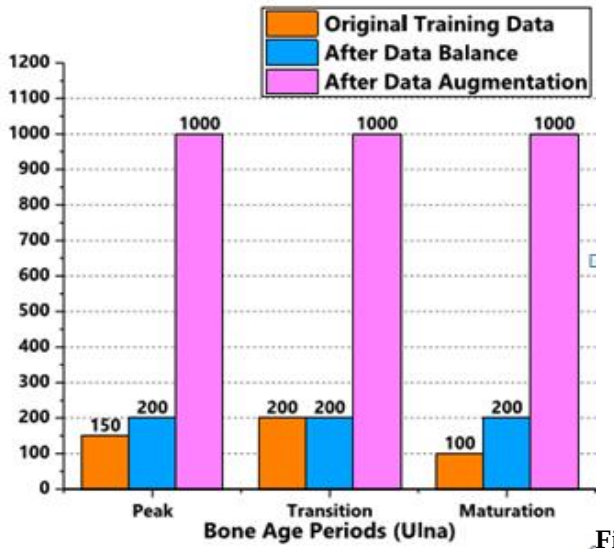

Fig 4(b): Data distributions after data balancing and augmentation (Ulna)

C. METHOD

The radiograph inputs to CNNs are too large to use directly. The important part to evaluate in the radiograph is the DRU region, which is only a small part of the input radiograph. Therefore, we use the object detection model, the Faster R-CNN, to extract the DRU region and reduce the unnecessary regions from the radiograph. From the detected image the DRU region was separated and resized to identical resolutions and then saved in a file and then use this data to train CNNs for bone age prediction. The bone age assessment method and architecture (Fig 5) are as follows:

➔ Preparation of data
➔ Reducing unnecessary regions and extracting DRU region from left hand radiograph using object detection model
➔ Cropping and resizing the DRU to the identical sizes
➔ Final Output

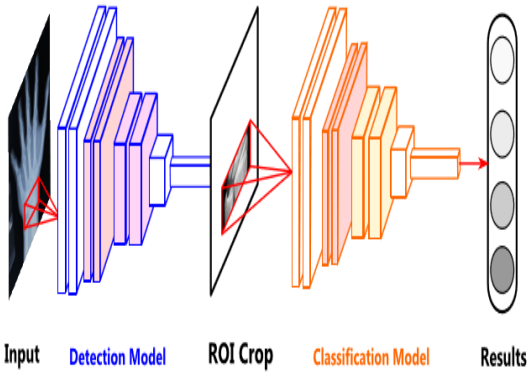

Fig 5: Architecture of an assessment of bone age method

The process, the assessment of bone age method follows is represent in the form of a flowchart as in the Fig 6. The flow chart gives us the brief idea of the flow of the input image processing, passing through the object detection model to find the ROI and resizing them, and then being sent to the CNN classification model for promising outputs.

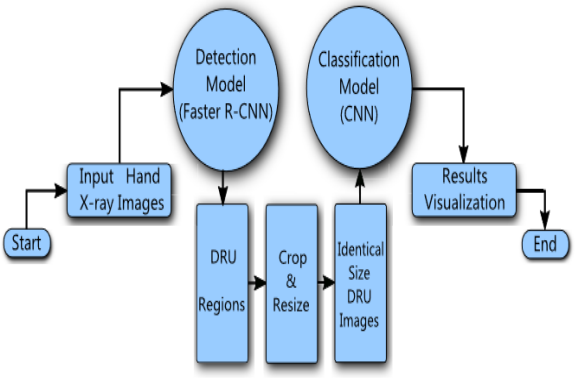

Fig 6: Flowchart for assessment of bone age method

ROI DETECTION

To extract the DRU from the input left hand radiographs, we use Faster R-CNN algorithm [20], an object detection model. ZF-Net [30], the basic algorithm that we use has 5 shareable CNNs. The first of the 5 has 7X7 sized 96 filters. The second of the 5 has 5X5 sized 256 filters with 3X3 of maximum pooling layer merged with the preceding layer. The max pooling layer in the approach followed with each convolutional layer. The next three 3X3 convolutional layers with 384, 384 and 256 respectively were made to follow the model the strides in this case were 1. And then another 3X3 convolutional layer was added followed by 2 sibling 1X1 convolutional layers. In the end the output will be the proposed region and bounding box scores. This above structure is called Region Proposal Network (RPN). An RPN obtains the appropriate region, which is called as Region of Interest, denoted as (ROI). This ROI and the layers of neural network were passed to the ROI pooling layer contains two distinct completely connected layers which are of 4096 size. Subsequently, we get the output as scores of region proposed and bounding box coordinates. This as a total is called as Faster R-CNN [31]. The object detection model used in the experiment is shown in the Fig 7. Back propagation and stochastic gradient descent (SGD) were used in training the model for detection of bone age and Gaussian distribution was utilized to initialize all the layer's weights and 0.01 was set as the learning rate. The training conducts as follows

- ➔ Training RPN which includes 8000 iterations
- ➔ Using 4000 iterations in order to have Faster R-CNNs.
- ➔ Step 1 and 2 are repeated again

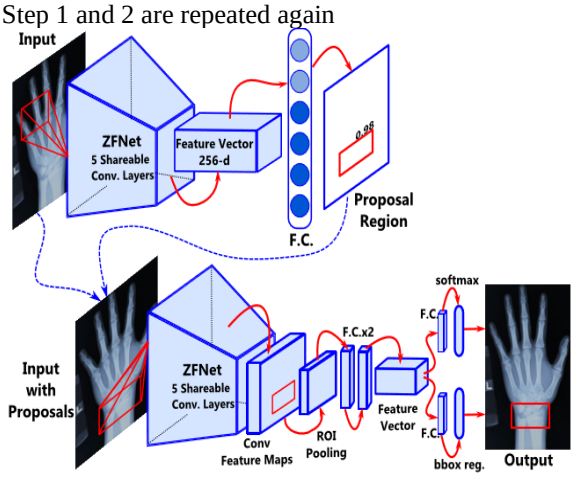

Fig 7: Faster R-CNN structure

CLASSIFICATION OF SKELETAL MATURITY

A CNN, multi layered Neural Network (Fig 8), Constitutes with an Input, Hidden and an Output Layers. Several convolutional layers (extracts input images features) and max pool layers (reduces the coordinates of its input data) followed by fully connected layers (chooses useful features and establishes mapping relations among previous layers). This experiment includes the input data of the DRU, 4 or 5 convolutional neural layers of sizes 7X7, 5X5, 3X3 or all 3X3. A 2X2 max pooling layer follows every convolutional layer. At the end fully connected layers of 4096 or 1024 were added with or without dropout [33]. Activation function used is ReLU. True and false positive (TP, FP) and true and false negative (TN, FN) are the parameters considered to calculate the accuracy of the model performance.

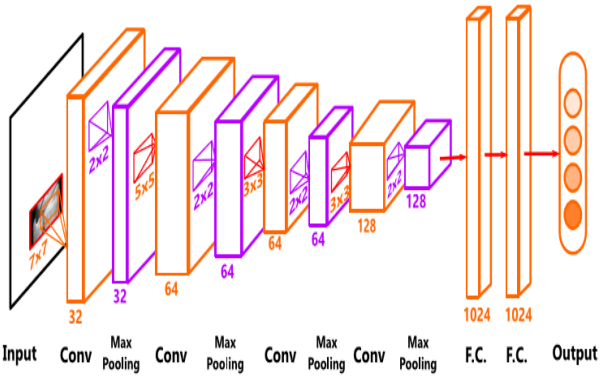

Fig 8: CNN Classification Method Structure

IV. EXPERIMENTAL RESULTS

A. CONFIGURATION OF AN EXPERIMENT

Ubuntu 16.04 system was used to implement this experiment. CPU is Intel R Xeon R CPU E5–1620 v3. 3.5GHz XPU frequency. NVIDIA Quadro M4000 GPU, CUDA8.0, cuDNN5.0. Caffe framework, based detection task and Theano based classification task and Lasagne Deep Learning framework were used. Adam optimization algorithm [34] (self-adapted parameters algorithm: learning rate (0.0001) and 2 decay (0.9, 0.999) parameters) and minimized multiple classification cross-entropy loss function were used in the training process. Xavier uniform distribution initializes the weight matrix and bias takes 0 as value. Mini-batch of size 16 were used to update the parameters.

B. CLASSIFICATION RESULTS

1. PERFORMANCE OF MODEL IN CASE OF BALANCED SAMPLES

We categorized the data as balanced and unbalanced data and compared the neural network performance in both the cases. The network used in this experiment consists of 4 convolutional layers (first layer 32 filters with size 7X7; Second layer 5X5 sized 64 filters, third layer 64 filters of 3X3 size and fourth layer 32 filters with size 3X3) and 2 fully connected layers of sizes 4096 and 1024 as per convenience. A max pool layer follows each convolutional layer and 3 was made to be the size of the output image. Fig 9 represents the results of the experiment.

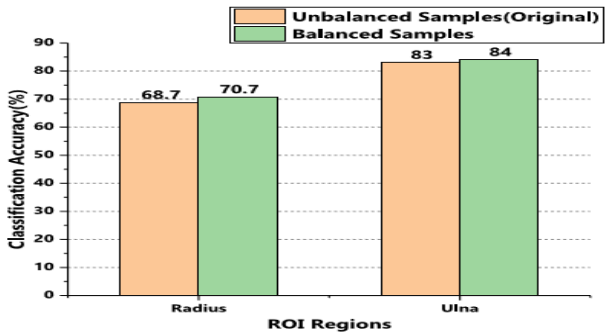

Fig 9: Comparison of neural network performance when fed with unbalanced and balanced datasets

We can observe the tiny accuracy improvement in case of the balanced data. The training procedure shows that the convergence speed was faster in balanced samples than that of unbalanced, where unbalanced data experiment converges after 40 iterations (Fig 10(a)), the balanced data experiment converges after 20 iterations (Fig 10(b)), thus proving that the data balancing was effective and time-saving.

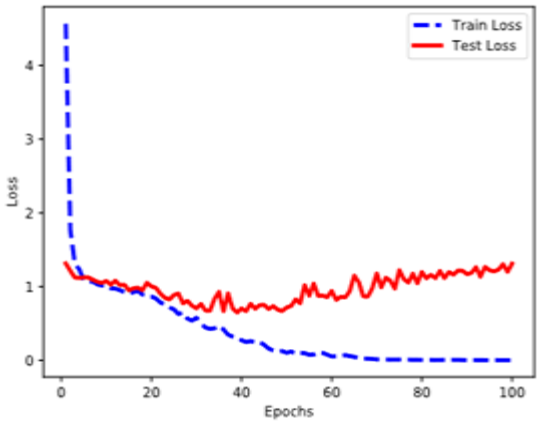

Fig 10(a): Convergence Speed Comparison of Balanced Datasets

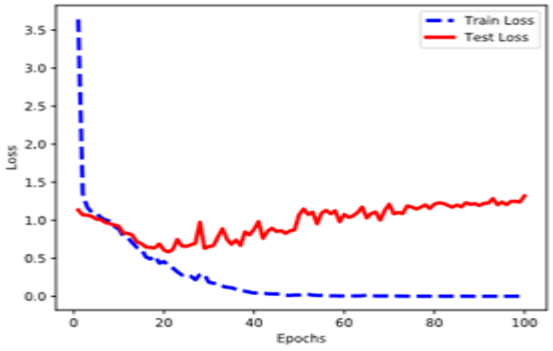

Fig 10(b): Convergence Speed Comparison of Unbalanced Datasets

2. PERFORMANCE OF MODEL IN CASE OF AUGMENTED DATA

In this study, to enlarge the dataset, rescaling and translations acted upon the data and increased data 5 times more (1000 images per group and total image count sets to 3000). Now comparing the performances of these described datasets using any rudimentary neural network consisting of the sufficing no. of layers- convolutional are 4, fully connected layers are 2, the obtained output is as represented in the Fig 11.

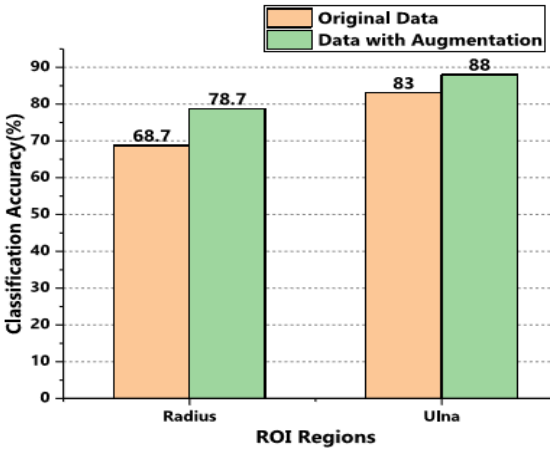

Fig 11: Comparison of neural network performance when fed with unbalanced and augmented datasets

Augmentation of the data improved the performance slightly and even better than the balanced dataset. It increased the model's convergence speed. The Fig 12(a),12(b) shows that when augmented data is fed to the models, the training loss is found decreasing considerably after following through just 10 iterations while ones fed with unbalanced datasets training loss reduces to zero after nearly 30 iterations.

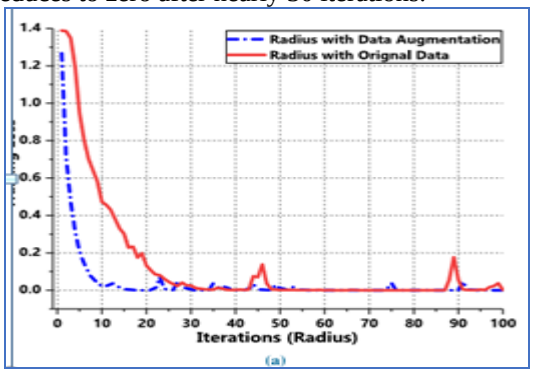

Fig 12(a): Training loss before and after data augmentation (Radius)

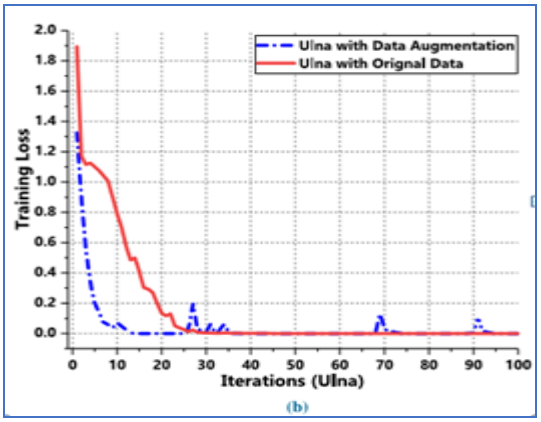

Fig 12(b): Training loss before and after data augmentation (Ulna)

3. PERFORMANCE OF MODEL WHEN VARIOUS CONFIGURATIONS WERE USED

Factors that influence the model performance like no. of neurons and convolutional layers; kernel sizes taken in the convolutional layers; dropout techniques are useful in determining the performance of the network model when various configurations were used. Output of comparison of the accuracy of 7 configurations in predicting the right is tabulated (Table 3).

Table 3: comparison of different network configurations

Net. No.	Network Configurations	
	Convolutional Layer	Fully-Connected Layer
1	32c7-64c5-64c3-32c3	1024-1024
2	32c3-64c3-64c3-32c3	1024-1024
3	32c3-64c3-64c3-128c3-128c3	4096-1024
4	32c7-64c5-64c3-128c3-128c3	1024-1024
5	32c5-64c5-64c5-128c3-128c3	1024-1024
6	32c5-64c5-64c5-128c3-128c3-128c3	4096-1024
7	32c3-64c3-64c3-128c3-128c3-128c3	1024-1024

For example: 32c5-64c3-64c3-32c3 represents 4 convolutional layers where the layers have 5X5 sized 32 filters, 3X3 sized 64 filters, 3X3 sized 64 filters, 3X3 sized 32 filters respectively. And 4096-1024 signifies the presence of 4096 and 1024 sized fully connected layers respectively. Adam optimization algorithm was used during the training procedure and 0.0001 was the rate of learning and 0.9 was the value of 1 decay parameter and 0.999 was the value that was set to the other decay parameter and Xavier distribution was used to initialize the weight matrix W and biases were initialized to zero. Fig 13(a),13(b) shows ulna and radius classification results. We can observe that the classification accuracy of the radius has its highest accuracy of 0.92 on third network classification on the other hand ulna of 0.90 on No. 4 network classification. This concludes that the higher classification accuracies aren't guaranteed by deeper networks and the right configuration for the classification of the distal radius and ulna region should come to a conclusion after diverse experiments and construction of networks, ones that utilize the techniques of dropout especially.

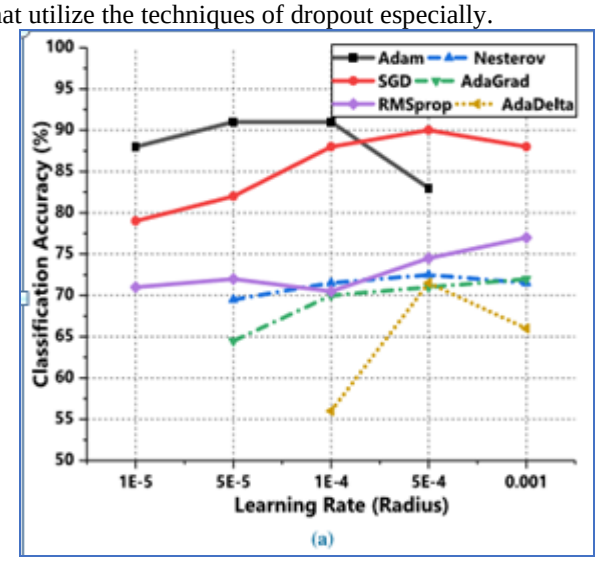

Fig 13(a): Classification Accuracy of Radius for various Optimization Algorithms.

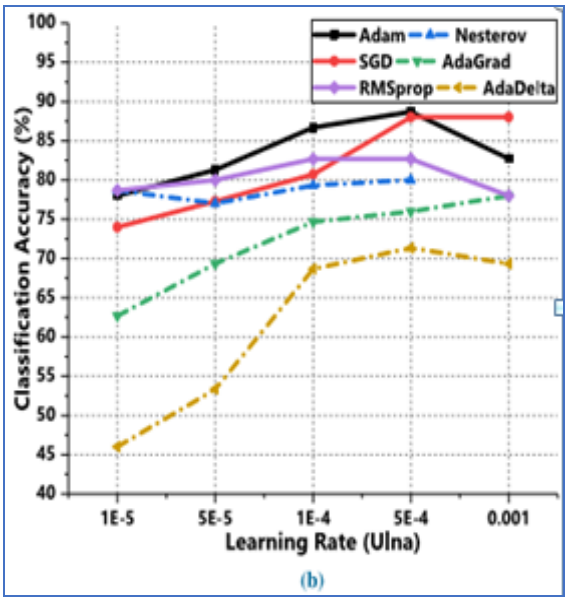

Fig 13(b): Classification Accuracy of Ulna for various Optimization Algorithms.

V. CONCLUSION

In the experiment, to improve the bone age assessment and assist clinical decisions of physicians, we trained a CNN with left hand and wrist and DRU to predict skeletal maturity. Classification result shows that the best performance of radius and ulna is 92% and 90%respectively. On the other side of the coin, the cons, we don't have adequate early growth stage data to train our model and the DRU region which includes some noise further it can be used for final prediction accuracy which makes the method little complicated. And the classification errors are analyzed with the usage of various confusion matrices. Coming to the future scope there is a need of more and more effective deep learning-based techniques must be implemented, in order to ignore the above-mentioned issues, say having more patient's features and used bigger and complicated networks so that the skeletal maturity/bone age assessment results are at its best

REFERENCES

1. J. P. Y. Cheung and K. D.-K. Luk, ''Managing the paediatric spine: Growth assessment,'' Asian Spine J., vol. 11, no. 5, pp. 804–816, 2017.
2. K. M. C. Cheung et al., ''Magnetically controlled growing rods for severe spinal curvature in young children: A prospective case series,'' Lancet, vol. 379, no. 9830, pp. 1967–1974, 2012.
3. M. Dominkus, P. Krepler, E. Schwameis, R. Windhager, and R. Kotz, ''Growth prediction in extendable tumor prostheses in children,'' Clin. Orthopaedics Rel. Res., vol. 390, pp. 212–220, Sep. 2001.
4. R. B. Duthie, ''The significance of growth in orthopaedic surgery,'' Clin. Orthopaedics Rel. Res., vol. 14, pp. 7–19, Jun. 1959.
5. G. H. Thompson, B. A. Akbarnia, and R. M. Campbell, Jr., ''Growing rod techniques in early-onset scoliosis,'' J. Pediatric Orthopaedics, vol. 27, no. 3, pp. 354–361, 2007.
6. K. D.-K. Luk, L. B. Saw, S. Grozman, K. M. Cheung, and D. Samartzis, ''Assessment of skeletal maturity in scoliosis patients to determine clinical management: A new classification scheme using distal radius and ulna radiographs,'' Spine J., vol. 14, no. 2, pp. 315–325, 2014.

7. W. W. Greulich and S. I. Pyle, ''Radiographic atlas of skeletal development of the hand and wrist,'' Amer. J. Med. Sci., vol. 238, no. 3, p. 393, 1959.
8. J. M. Tanner and R. H. Whitehouse, ''Clinical longitudinal standards for height, weight, height velocity, weight velocity, and stages of puberty,'' Arch. Disease Childhood, vol. 51, no. 3, pp. 170–179, 1976.
9. J. M. Tanner, R. H. Whitehouse, P. C. R. Hughes, and B. S. Carter, ''Relative importance of growth hormone and sex steroids for the growth at puberty of trunk length, limb length, and muscle width in growth hormonedeficient children,'' J. Pediatrics, vol. 89, no. 6, pp. 1000–1008, 1976.
10. J. M. Tanner, R. H. Whitehouse, E. Marubini, and L. F. Resele, ''The adolescent growth spurt of boys and girls of the Harpenden growth study,'' Ann. Hum. Biol., vol. 3, no. 2, pp. 109–126, 1976.
11. J. P. Y. Cheung, D. Samartzis, P. W. H. Cheung, K. M. Cheung, and K. D.-K. Luk, ''Reliability analysis of the distal radius and ulna classification for assessing skeletal maturity for patients with adolescent idiopathic scoliosis,'' Global Spine J., vol. 6, no. 2, pp. 164–168, 2016.
12. J. P. Y. Cheung, D. Samartzis, P. W. H. Cheung, K. H. Leung, K. M. C. Cheung, and K. D.-K. Luk, ''The distal radius and ulna classification in assessing skeletal maturity: A simplified scheme and reliability analysis,'' J. Pediatric Orthopaedics B, vol. 24, no. 6, pp. 546–551, 2015.
13. J. P. Y. Cheung, P. W. H. Cheung, D. Samartzis, K. M. C. Cheung, and K. D.-K. Luk, ''The use of the distal radius and ulna classification for the prediction of growth: Peak growth spurt and growth cessation,'' Bone Joint J., vol. 98, no. 12, pp. 1689–1696, 2016.
14. J. P. Y. Cheung, P. W. H. Cheung, D. Samartzis, and K. D.-K. Luk, ''Curve progression in adolescent idiopathic scoliosis does not match skeletal growth,'' Clin. Orthopaedics Rel. Res., vol. 476, no. 2, pp. 429–436, 2017.
15. H. Greenspan, B. V. Ginneken, and R. M. Summers, ''Guest editorial deep learning in medical imaging: Overview and future promise of an exciting new technique,'' IEEE Trans. Med. Imag., vol. 35, no. 5, pp. 1153–1159, Mar. 2016.
16. M. Anthimopoulos, S. Christodoulidis, L. Ebner, A. Christe, and S. Mougiakakou, ''Lung pattern classification for interstitial lung diseases using a deep convolutional neural network,'' IEEE Trans. Med. Imag., vol. 35, no. 5, pp. 1207–1216, May 2016.
17. P. Liskowski and K. Krawiec, ''Segmenting retinal blood vessels with deep neural networks,'' IEEE Trans. Med. Imag., vol. 35, no. 11, pp. 2369–2380, Nov. 2016.
18. A. A. A. Setio et al., ''Pulmonary nodule detection in CT images: False positive reduction using multi-view convolutional networks,'' IEEE Trans. Med. Imag., vol. 35, no. 5, pp. 1160–1169, May 2016.
19. H. Lee et al., ''Fully automated deep learning system for bone age assessment,'' J. Digit. Imag., vol. 30, no. 4, pp. 427–441, 2017.
20. S. Ren, K. He, R. Girshick, and J. Sun, ''Faster R-CNN: Towards realtime object detection with region proposal networks,'' IEEE Trans. Pattern Anal. Mach. Intell., vol. 39, no. 6, pp. 1137–1149, Jun. 2017.
21. A. Tristán-Vega and J. I. Arribas, ''A radius and ulna TW3 bone age assessment system,'' IEEE Trans. Biomed. Eng., vol. 55, no. 5, pp. 1463–1476, May 2008.
22. J. Liu, J. Qi, Z. Liu, Q. Ning, and X. Luo, ''Automatic bone age assessment based on intelligent algorithms and comparison with TW3 method,'' Comput. Med. Imag. Graph., vol. 32, no. 8, pp. 678–684, 2008.
23. K. Somkantha, N. Theera-Umpon, and S. Auephanwiriyakul, ''Bone age assessment in young children using automatic carpal bone feature extraction and support vector regression,'' J. Digit. Imag., vol. 24, no. 6, pp. 1044–1058, 2011.
24. H.-H. Lin, S.-G. Shu, Y.-H. Lin, and S.-S. Yu, ''Bone age cluster assessment and feature clustering analysis based on phalangeal image rough segmentation,'' Pattern Recognit., vol. 45, no. 1, pp. 322–332, 2012.
25. J. Seok, B. Hyun, J. Kasa-Vubu, and A. Girard, ''Automated classification system for bone age X-ray images,'' in Proc. IEEE Int. Conf. Syst., Man, Cybern. (SMC), Oct. 2012, pp. 208–213.
26. L. M. Davis, B-J. Theobald, and A. Bagnall, ''Automated bone age assessment using feature extraction,'' in Proc. Int. Conf. Intell. Data Eng. Autom. Learn., 2012, pp. 43–51.
27. M. Harmsen, B. Fischer, H. Schramm, T. Seidl, and T. M. Deserno, ''Support vector machine classification based on correlation prototypes applied to bone age assessment,'' IEEE J. Biomed. Health Informat., vol. 17, no. 1, pp. 190–197, Jan. 2013.
28. P. Cunha, D. C. Moura, M. A. G. López, C. Guerra, D. Pinto, and I. Ramos, ''Impact of ensemble learning in the assessment of skeletal maturity,'' J. Med. Syst., vol. 38, no. 9, p. 87, 2014.
29. T. Ebner, D. Stern, R. Donner, H. Bischof, and M. Urschler, ''Towards automatic bone age estimation from MRI: Localization of 3D anatomical landmarks,'' in Proc. Int. Conf. Med. Image Comput. Comput.-Assist. Intervent., 2014, pp. 421–428.
30. M. D. Zeiler and R. Fergus, ''Visualizing and understanding convolutional networks,'' in Proc. Eur. Conf. Comput. Vis., 2014, pp. 818–833.
31. R. Girshick. (2015). ''Fast R-CNN.'' [Online]. Available: https://arxiv.org/ abs/1504.08083
32. K. Simonyan and A. Zisserman. (2014).''Very deep convolutional networks for large-scale image recognition.'' [Online]. Available: https:// arxiv.org/abs/1409.1556
33. N. Srivastava, G. Hinton, A. Krizhevsky, I. Sutskever, and R. Salakhutdinov, ''Dropout: A simple way to prevent neural networks from overfitting,'' J. Mach. Learn. Res., vol. 15, no. 1, pp. 1929–1958, 2014.
34. D. P. Kingma and J. Ba. (2014). ''Adam: A method for stochastic optimization.'' [Online]. Available: https://arxiv.org/abs/1412.6980
35. G. E. Güraksın, H. Haklı, and H. Uguz, ''Support vector machines classifi- ˇ cation based on particle swarm optimization for bone age determination,'' Appl. Soft Comput., vol. 24, pp. 597–602, Nov. 2014.

AUTHORS PROFILE

Ms. B Sowmya Reddy is currently pursuing B.Tech Degree program in Computer Science & Engineering in Sreenidhi Institute of Science and Technology, Affiliated to Jawaharlal Nehru Technical University Hyderabad, Telangana, India. Her main research work focuses on Medical Image Processing, Machine Learning and Neural Networks

Mr. Devevarapu Sreenivasarao, currently working as an Assistant Professor in the department of CSE in Sreenidhi Institute of Science and Technology since 2014. He did Master of Technology from JNT University Hyderabad, India in year 2012. He is a research scholar in Annamalai University which was located in Chidambaram, Tamilnadu, India He has published more than 15 research papers in various peer reputed international journals..His main research work focuses on Medical Image Processing, Machine Learning.

Mr. Shaik Khasim Saheb currently working as an assistant Professor in the department of CSE in Sreenidhi Institute of Science and Technology since 2014. He did masters from VIT University, Tamilnadu, India. 2014. He is a research scholar in Annamalai University which was located in Chidambaram, Tamilnadu, India. He has published more than 10 research papers in various peer reputed international journals. His main research work focuses on Medical Image Processing, Machine Learning.

Published By:
Blue Eyes Intelligence Engineering and Sciences Publication (BEIESP)